# Exploitation of the CEOS Pseudo Invariant Calibration Sites (PICS) for Vicarious Calibration of Optical Imagers

## CEOS/WGCV/IVOS n°31 presentation: review of the study

ESA: M. Bouvet
Consortium: NOVELTIS: C.Bacour, L. Grignon, E. Munesa
ONERA: F. Viallefont-Robinet, X. Briottet, Y. Boucher, F. Lemaître, T. Rivière
LSCE: F.-M. Bréon

# Outline

- **Context & objectives**
- Sites selection process
- Surface characterization
- Atmospheric characterization
- PICSAND Data Base
- Conclusion

# Context & objectives

- Revisit the list of Pseudo-Invariant Calibration Sites (PICS) over desert areas defined 20 years ago by Cosnefroy et al. (1996) based on more recent multi-spectral remote sensing data with enhanced temporal and spatial coverages and resolutions

- Collect sand samples from an ensemble of identified sites and measure in laboratory their physical (mineralogy and grain size distribution) and optical (spectro-directional reflectance) properties

- Build a database combining the sand optical properties estimated from the sampled collected with other databases available in the literature

- Build a climatology of aerosol optical properties over the PICS selected, combined with other atmospheric variables

- Summarize the PICS characterisation results and provide final recommendations.

# Outline

- Context & objectives
- **Sites selection process**
- Surface characterization
- Atmospheric characterization
- PICSAND Data Base
- Conclusion

# Sites selection process

- **Criteria:**
  - **temporal stability** of their optical properties (< 4% as a starting value)
  - **spatial homogeneity** (< 3% as a starting value)
  - weak / well characterized directional effects
  - weak cloud cover and low aerosol load and well characterized aerosol type
  - proximity of meteorological / AERONET stations
  - importance/relevance wrt other CEOS cal/val activities
  - accessibility

# Sites selection process

- **Process:**

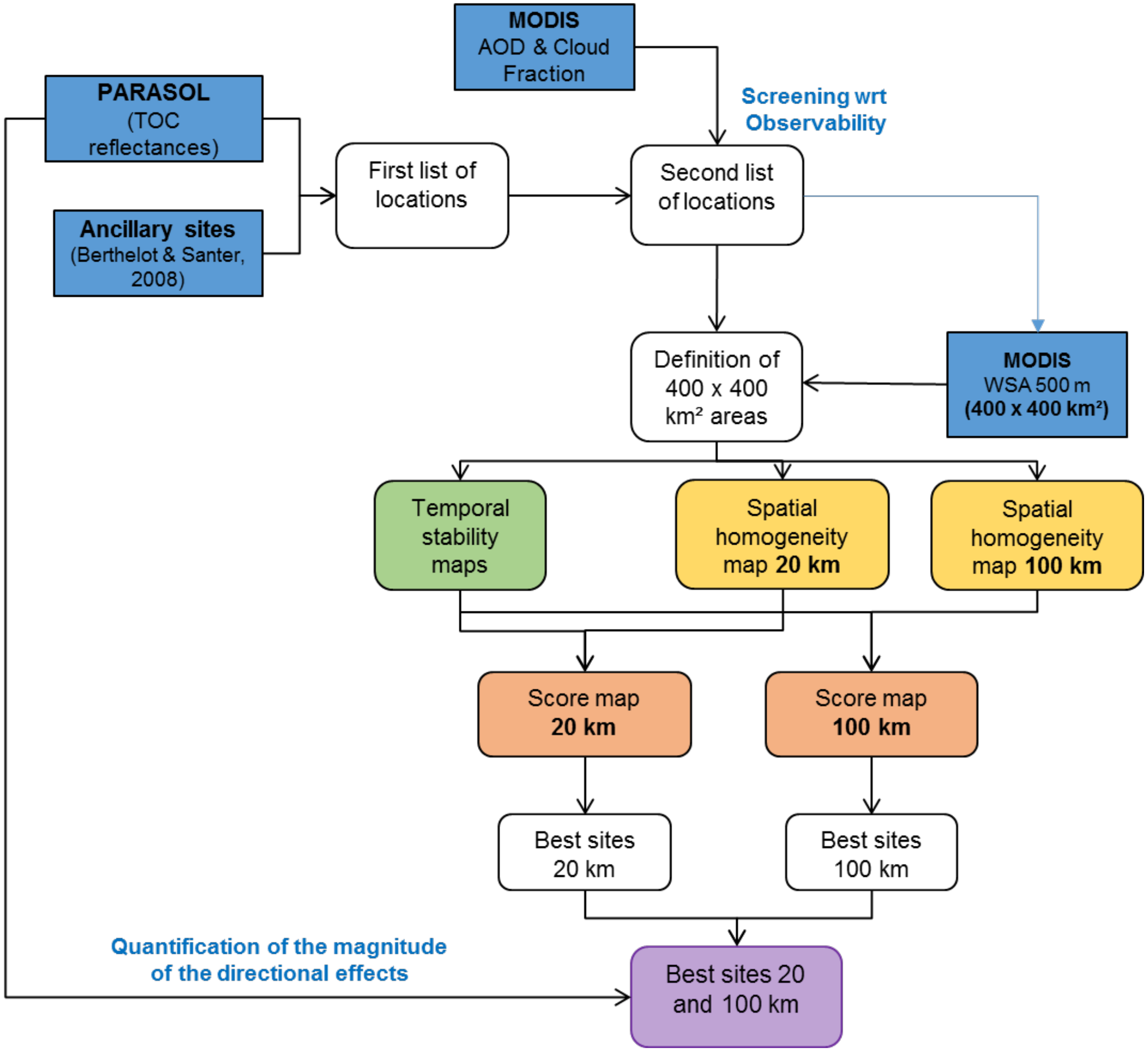

# Sites selection process

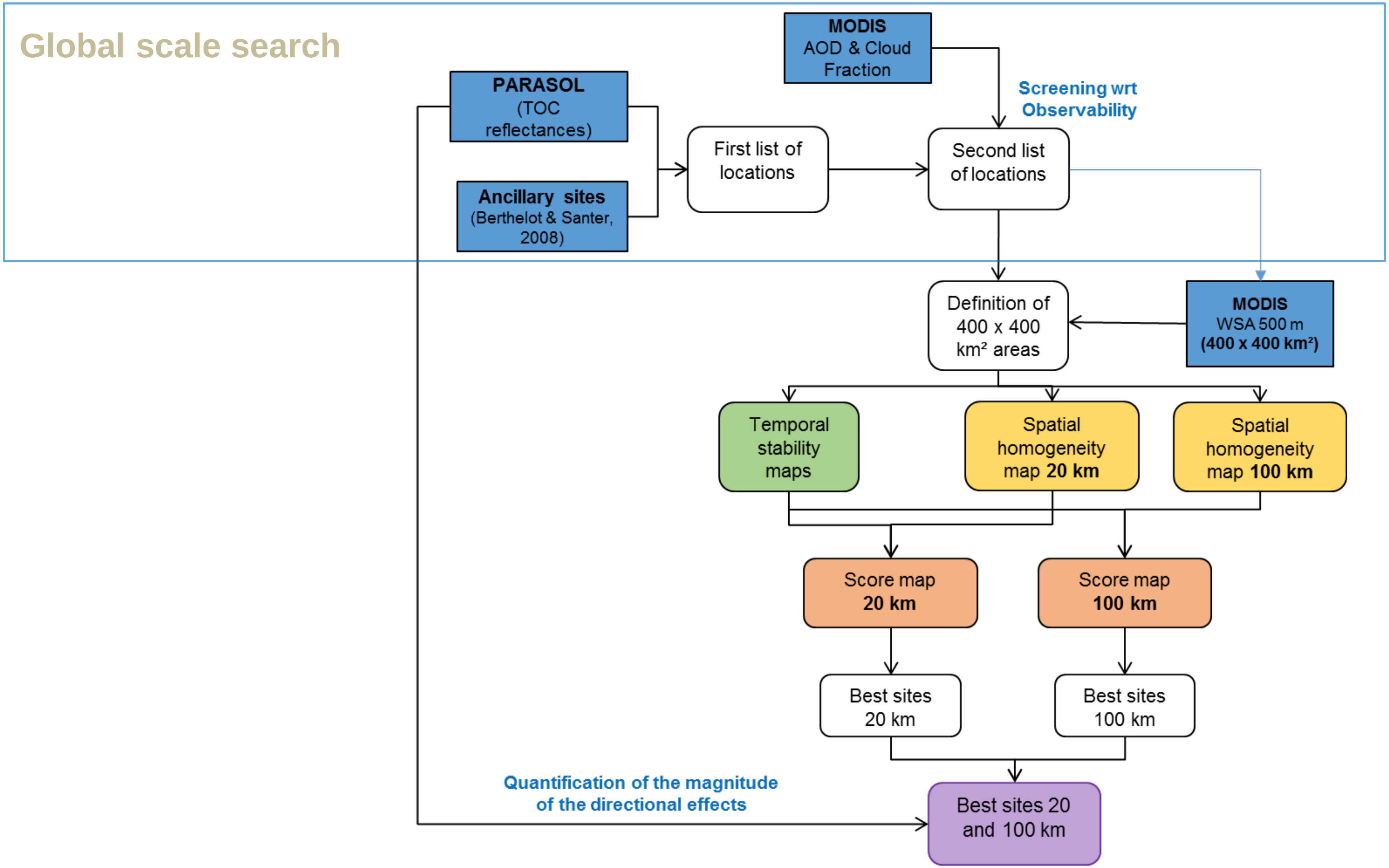

# Processing Global Scale

## Ancillary sites

•Candidate locations used in Rad/Cal activities (**Berthelot and Santer, 2008)**

**PARASOL**
**93 candidate locations (red)**

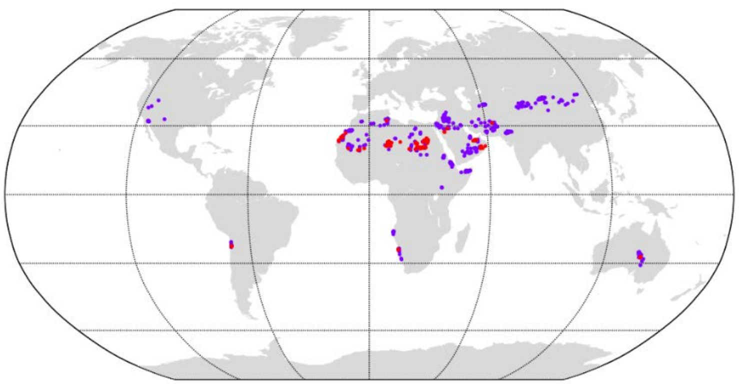

**79 ancillary locations (red)**

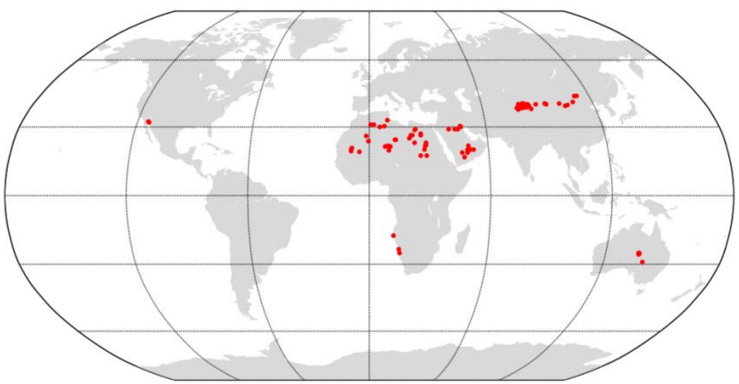

screening wrt (MODIS MYD04_L2)
- AOD
- Cloud Fraction

**identification of**
**125 possible locations**

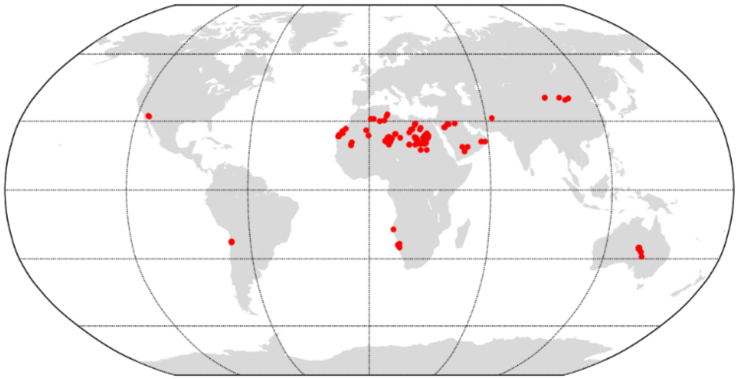

# Sites selection process

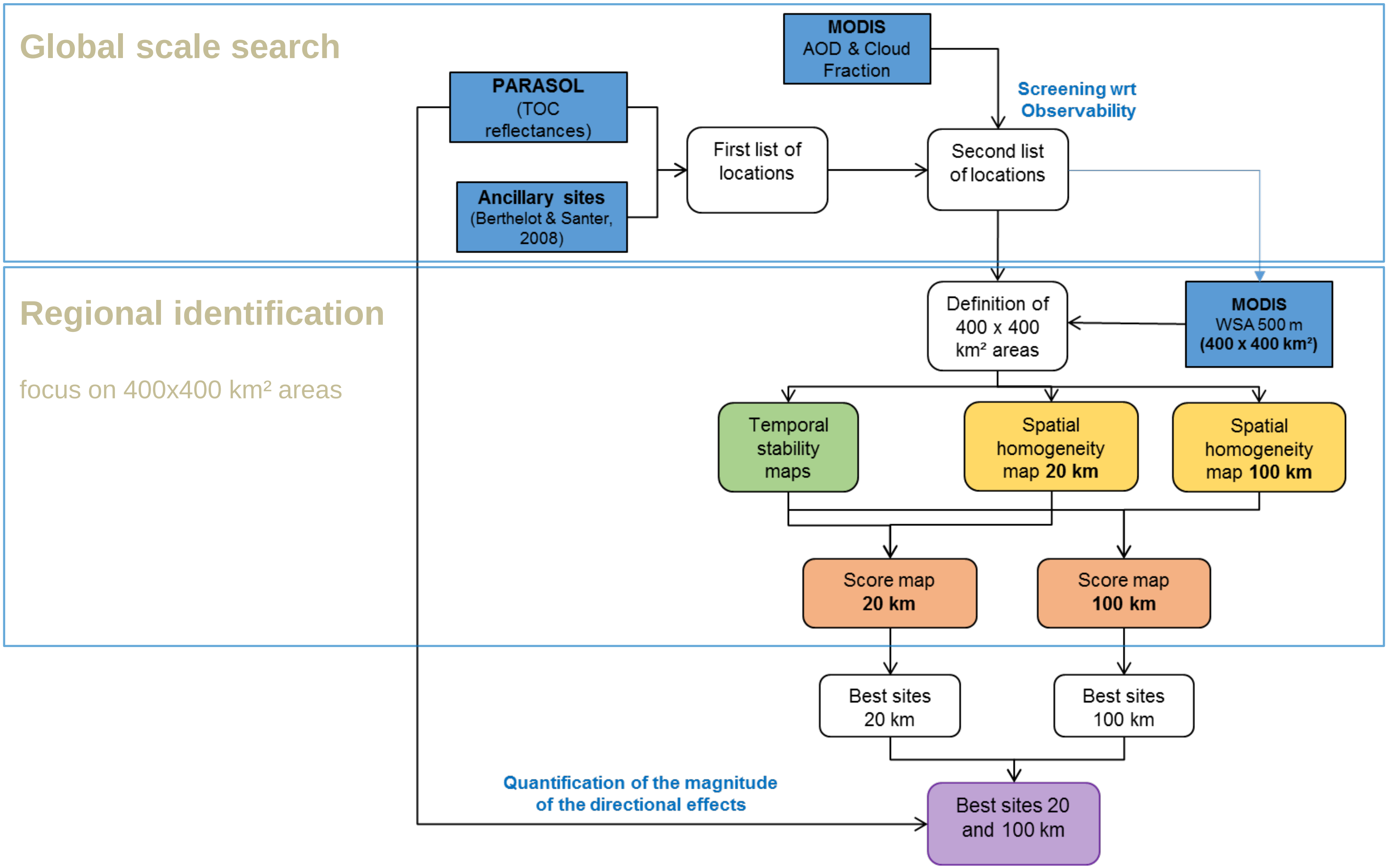

## Processing

**Temporal stability:** $TVar\lambda = \sigma\left(\rho_\lambda - \overline{\rho_\lambda}\right)/\overline{\rho_\lambda}$

**Spatial homogeneity**: $homog = \sigma(\rho_n)/\overline{\rho_n}$ (moving windows of size = 20x20 and 100x100 km²)

**Score at 20/100/20+100 km**:

$$Score_{20km} = 2 * \overline{TVar_{\lambda,20km}} + homog_{20km}$$
$$Score_{100km} = 2 * \overline{TVar_{\lambda,100km}} + homog_{100km}$$
$$Score_{20+100km} = Score_{20km} + Score_{100km}$$

# Sites selection process

## Spatial homogeneity – 20 km

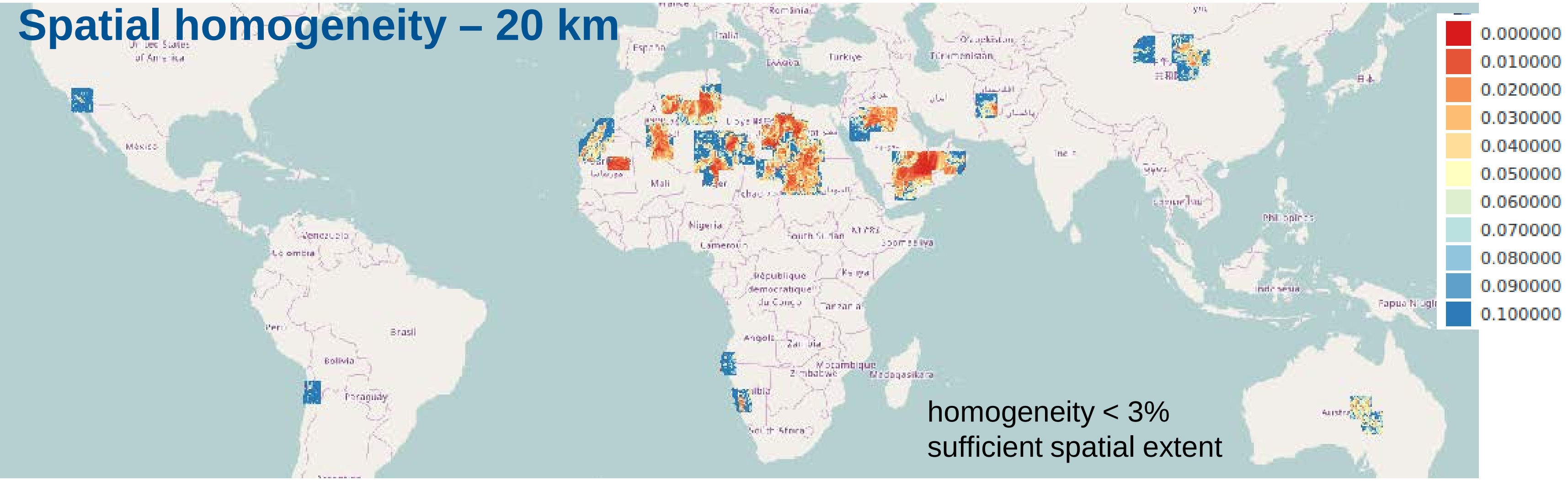


## Temporal stability

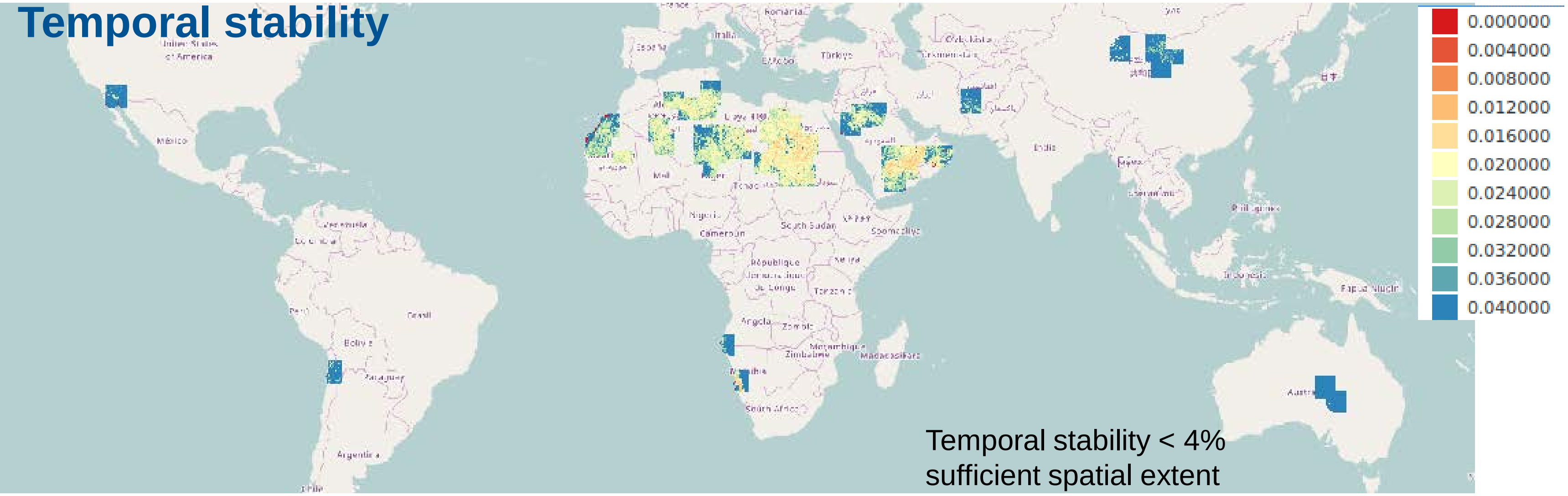

## Sites after regional identification:

- **20 sites close to Cosnefroy's ones**
- **Algeria**: 2 sites; scores within the 25th percentile wrt Cosnefroy sites; below for the optimal locations around Cosnefroy sites
- **Arabia**: 3 sites. Not as good as Arabia2, but superior to Arabia1
- **China**: too low spatial homogeneity ➔ no site
- **Libya**: sites identified with scores > Libya4 but with lower spatial homogeneity
- **Mauritania**: 1 site north-east of Mauritania1 with slightly better scores
- **Namibia**: 1 site relevant for 20 km applications. One of the best score found among all sites. Location about 162 km south-east of Gobabeb

## Ranking of Cosnefroy's sites

| Score 20 km | |
|---|---|
| **Cosnefroy site** | **Optimal location** |
| Arabia2 [ 20.13°, 50.96°] (0.034) | Arabia2 [ 20.51°, 51.80°] (0.029) |
| Sudan1 [ 21.74°, 28.22°] (0.039) | Libya3 [ 22.79°, 23.46°] (0.032) |
| Arabia1 [ 18.88°, 46.76°] (0.046) | Arabia1 [ 19.83°, 47.06°] (0.033) |
| **Mauritania2** [ 20.85°, -8.78°] (0.049) | Sudan1 [ 21.60°, 27.37°] (0.034) |
| Libya2 [ 25.05°, 20.48°] (0.050) | Algeria4 [ 30.41°, 5.25°] (0.040) |
| **Libya4** [ 28.55°, 23.39°] (0.050) | Egypt1 [ 26.45°, 26.59°] (0.042) |
| Egypt1 [ 27.12°, 26.10°] (0.050) | Libya2 [ 24.86°, 20.74°] (0.044) |
| **Algeria3** [ 30.32°, 7.66°] (0.050) | **Mauritania2** [ 20.97°, -8.42°] (0.044) |
| **Mauritania1** [ 19.40°, -9.30°] (0.052) | **Mauritania1** [ 20.09°, -8.52°] (0.045) |
| **Libya1** [ 24.42°, 13.35°] (0.052) | Niger1 [ 20.32°, 9.67°] (0.045) |
| **Algeria5** [ 31.02°, 2.23°] (0.054) | **Algeria3** [ 31.32°, 7.77°] (0.046) |
| Algeria1 [ 23.80°, -0.40°] (0.055) | Algeria1 [ 23.98°, -0.82°] (0.047) |
| Algeria4 [ 30.04°, 5.59°] (0.055) | **Libya1** [ 24.98°, 14.36°] (0.047) |
| Niger2 [ 21.37°, 10.59°] (0.055) | Mali1 [ 19.60°, -5.87°] (0.047) |
| Niger1 [ 19.67°, 9.81°] (0.055) | Algeria2 [ 25.76°, -0.31°] (0.048) |
| Mali1 [ 19.12°, -4.85°] (0.061) | **Libya4** [ 28.64°, 23.45°] (0.048) |
| Niger3 [ 21.57°, 7.96°] (0.062) | Arabia3 [ 28.78°, 43.42°] (0.049) |
| Algeria2 [ 26.09°, -1.38°] (0.069) | **Algeria5** [ 31.49°, 1.62°] (0.049) |
| Libya3 [ 23.15°, 23.10°] (0.071) | Niger2 [ 21.58°, 10.09°] (0.050) |
| Arabia3 [ 28.92°, 43.73°] (0.113) | Niger3 [ 22.03°, 7.35°] (0.057) |

# Sites selection process

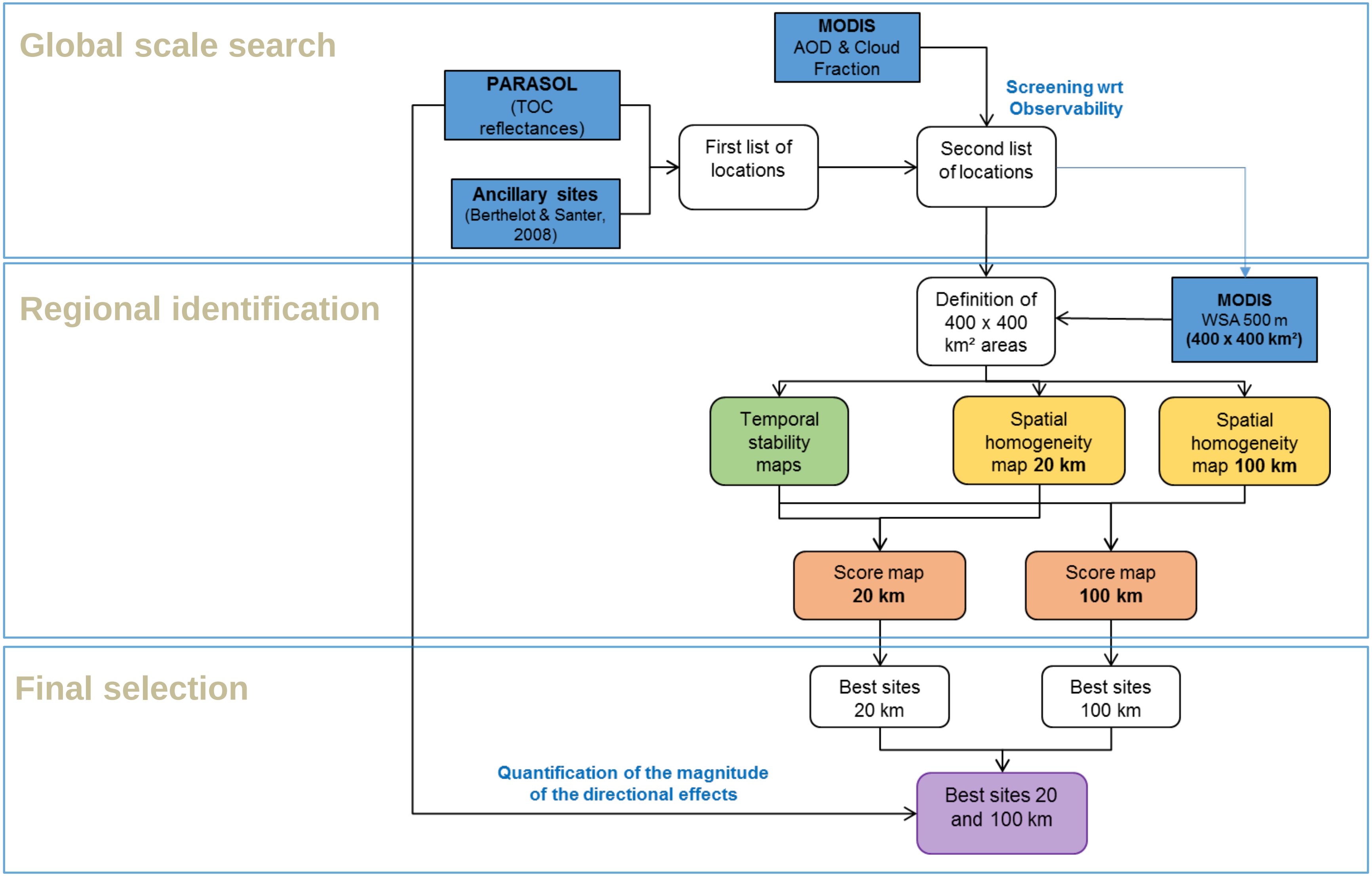

# Sites selection process

- Considering the accessibility (logistically speaking) of the sites identified in the first part of the study, and the importance of already existing ones with respect to Cal/Val activities, the selected sites for further characterization are:

  - The 6 IVOS sites widely used:
    **- Algeria3** and **Algeria5**;
    **- Libya1** and **Libya4;**
    **- Mauritania1** and **Mauritania2,**

  - New sites identified in this study:
    - One site in Namibia: **Namibia_PICSAND**;
    - One site in Arabia: **Arabia_PICSAND.**

# Outline

- Context & objectives
- Sites selection process
- **Surface characterization**
- Atmospheric characterization
- PICSAND Data Base
- Conclusion

# Overview of the samples

| Sample | Decimal geographic coordinates | Site nearby | Kind of meas. | Mineralogy | Grain size distribution |
|---|---|---|---|---|---|
| ONERA_Algeria3_PICSCEOS | 29.34 N / 7.33 E | Algeria3 | spectro-directional | yes | yes |
| ONERA_Algeria4_PICSCEOS | 29.84 N / 5.78 E | Algeria4 | spectro-directional | yes | yes |
| ONERA-Bristow_Algeria5_PICSCEOS_SPL1 | 30.5783 N / 2.3468 E | Algeria5 | spectro-directional | yes | yes |
| ONERA-Bristow_Algeria5_PICSCEOS_SPL2 | 30.5920 N / 2.1012 E | Algeria5 | spectro-directional | yes | yes |
| ONERA-Bristow_Algeria5_PICSCEOS_SPL3 | 30.7344 N / 2.7814 E | Algeria5 | spectro-directional | yes | yes |
| ONERA-ESA_Arabia_PICSAND_SPL1 | 29.4823 N / 41.1445 E | Arabia | spectro-directional | yes | yes |
| ONERA-ESA_Arabia_PICSAND_SPL2 | 29.4791 N / 41.1401 E | Arabia | spectro-directional | yes | yes |
| ONERA-ESA_Arabia_PICSAND_SPL3 | 29.4404 N / 41.1710 E | Arabia | spectro-directional | yes | yes |
| ONERA-ESA_Arabia_PICSAND_SPL4 | 29.4403 N / 41.1708 E | Arabia | spectro-directional | yes | yes |
| ONERA-ESA_Arabia_PICSAND_SPL5 | 29.4394 N / 41.1700 E | Arabia | spectro-directional | yes | yes |
| ONERA-ESA_Arabia_PICSAND_SPL6 | 29.33475 N / 41.3207 E | Arabia | spectro-directional | yes | yes |
| ONERA-White_Namibia_LUD1 | -26.6849 N / 15.2071 E | Namibia | spectral | yes | yes |
| ONERA-White_Namibia_LUD3 | -26.7245 N / 15.3104 E | Namibia | spectral | yes | yes |
| ONERA-White_Namibia_SOSS2 | -24.7234 N / 15.3174 E | Namibia | spectral | yes | yes |
| ONERA-White_Namibia_SOSS10 | -24.4578 N / 15.7765 E | Namibia | spectral | yes | yes |
| ONERA_Namibia_Gobabeb_Dunes | -23.5699 N / 15.0434 E | | spectro-directional | yes | yes |
| ONERA-CNES_Namibia_RadCalNet | | | spectro-directional | yes | yes |
| ONERA-Lau_Australia_PIN01 | -30.5900 N / 115.15675 E | | spectral | yes | no |
| ONERA-Lau_Australia_PIN02 | -30.5846 N / 115.1496 E | | spectral | yes | yes |
| ONERA-Lau_Australia_PIN03 | -30.5844 N / 115.1492 E | | spectral | yes | no |
| ONERA-Lau_Australia_PIN04 | -30.5824 N / 115.1468 E | | spectral | yes | no |
| ONERA-Lau_Australia_PIN05 | -30.5810 N / 115.1452 E | | spectral | yes | yes |
| ONERA-Lau_Australia_PIN06 | -30.5829 N / 115.1472 E | | spectral | yes | yes |
| ONERA-Lau_Australia_Lucky_Bay | -33.9877 N / 122.2308 E | | spectral | no | no |
| ONERA-Lau_Australia_Wylie_Bay | -33.8247 N / 121.9975 E | | spectral | yes | yes |
| ONERA-Schaepman_Libya_Erg_Ubari | | | spectro-directional | yes | yes |
| ONERA-Bristow_Libya_Fezzan_Fezz | | | spectral | yes | yes |
| ONERA-Bristow_Morocco_Erg_Chebbi | | | spectro-directional | yes | yes |
| ONERA_Niger_Niamey | | | spectro-directional | yes | yes |
| ONERA-Thome_USA_Rail_Road_Valley | | | spectral | yes | yes |
| ONERA-Thome_USA_White_Sands | | | spectral | yes | yes |

- Grain size distribution

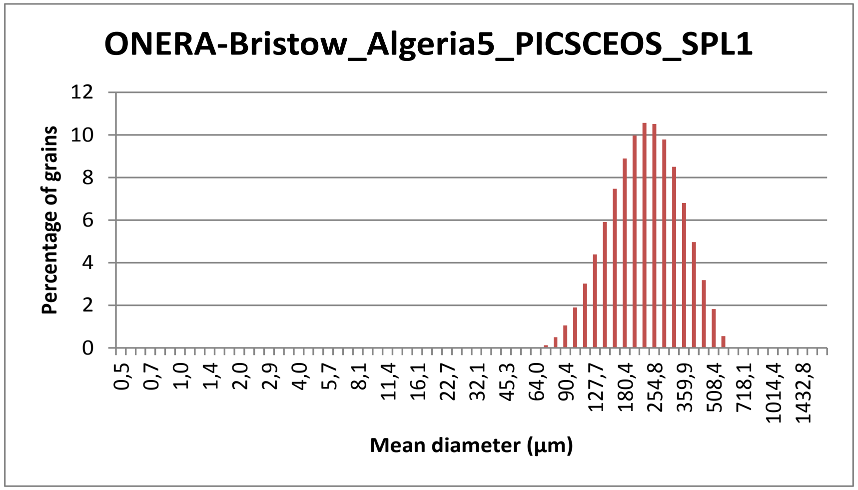


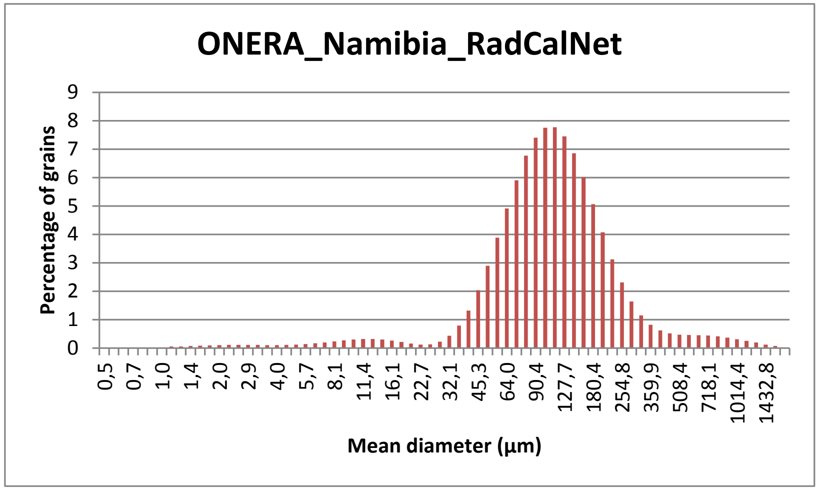


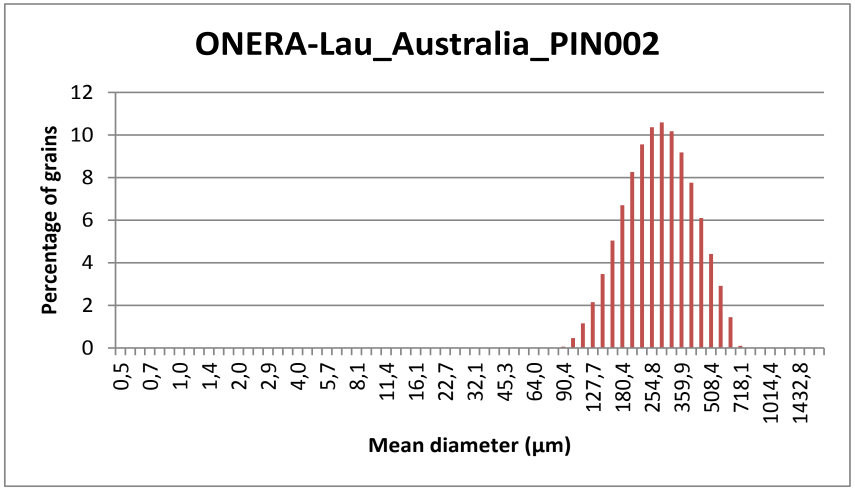


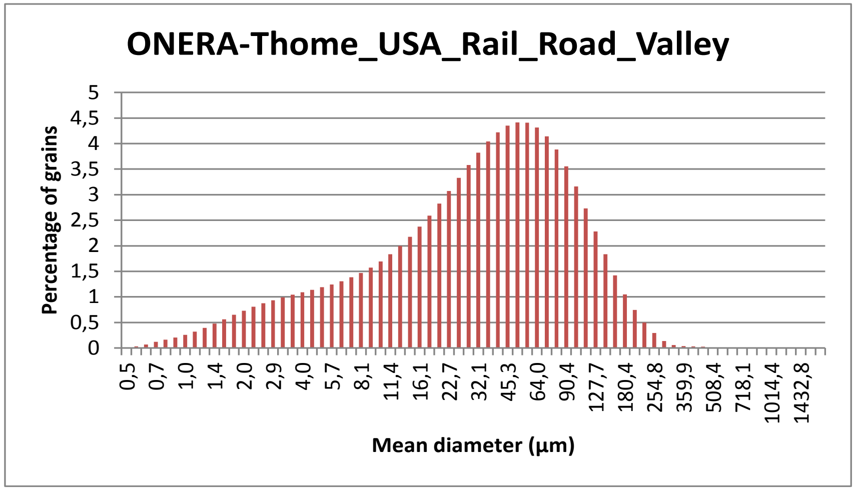

- Mineralogy
  - Qualitative: for all samples, performed by GEOPS thanks to X ray technique

| Sample name | Mineralogy (decreasing abundance order) |
|---|---|
| ONERA-Bristow_Algeria5_PICSCEOS_SPL1 | QUARTZ, Nitratine, Periclase, Spinel, Danalite, Dolomite, Rhomboclase |
| ONERA-Lau_Australia_PIN01 | QUARTZ, Fluorite, Halite, Aragonite, Pseudobrookite, Eglestonite, Calcite, Talc, Sperrylite, Calcite-Mg |
| ONERA-Lau_Australia_PIN02 | Aragonite, Quartz, Calcite-Mg, Calcite, Nitratine, Pyroxene, Topaz, Fluoro-eckermannite |
| ONERA-Lau_Australia_PIN03 | QUARTZ, Nitratine, Calcite, Aragonite, Clinoenstatite, Cristobalite, Perovskite-Nb, Lazulite, Marialite |
| ONERA-Lau_Australia_PIN04 | QUARTZ, Periclase, Nitratine, Cristobalite, Quartz, Cuprorhodsite, Moganite, Romeite, Hentschelite, Talc |
| ONERA-Lau_Australia_PIN05 | Aragonite, Quartz, Calcite-Mg, Calcite, Sylvite, Dolomite, Leucite |
| ONERA-Lau_Australia_PIN06 | QUARTZ, Aragonite, Calcite-Mg, Calcite, Lazulite, Marialite, Talc |
| ONERA-Lau_Australia_Wylie_Bay | Aragonite, Quartz, Calcite-Mg, Calcite, Anorthite-Na, Dolomite, Tremolite, Monetite, Feldspar |
| ONERA-CNES_Namibia_RadCalNet | Quartz, Albite, Diopside, Calcite, Dolomite, Ferrocolumbite, Muscovite, Feldspar, Apatite-Sr, Vanadinite, Chlorite |
| ONERA-Thome_USA_Rail_Road_Valley | Analcime, Halite, Quartz, Pyroxene, Almandine, Sodalite, Calcite, Phengite, Kaolinite, Albite |
| ONERA-Thome_USA_White_Sands | Gypsum, Anhydrite, Astrophyllite, Chabazite, Enstatite, Nitratine |

# Physical properties

- Mineralogy
  - Quantitative: for 17 samples, performed by BRGM (the geological French suvey) using X-ray diffractometry

**ONERA-Bristow_Algeria5_PICSCEOS_SPL1**

| Phases | weight % | Error (weight %) |
|---|---|---|
| Quartz | 97 | 3 |
| Potassium feldspar (microcline and/or orthose) | 2 | 3 |
| Kaolinite | 1 | 5 |

**ONERA-CNES_Namibia_Gobabeb_RadCalNet**

| Phases | weight % | Error (weight %) |
|---|---|---|
| Quartz | 46 | 3 |
| Plagioclase (albite on the diffractogram) | 19 | 3 |
| Potassium feldspar (microcline and/or orthose) | 14 | 3 |
| Illite and/or micas | 10 | 5 |
| Calcite | 5 | 3 |
| Amphibole (tremolite on the diffractogram) | 4 | 3 |
| Chlorite | 2 | 5 |
| Kaolinite | In traces | |

## Objectives

- Evaluated the capabilities of several semi-empirical models to fit:
  - the directional BCRF measurements performed in this study
  - bi-directional reflectance observations of PARASOL over the selected PICS
- Guide users for modeling of TOC/TOA reflectances over PICS

## Semi-empirical BRDF models

| Model name | Number of parameters | Parameter dependency |
|---|---|---|
| Hapke 1993 | 6 | non linear |
| Hapke 2002 | 6 | non linear |
| Hapke 2008 | 7 | non linear |
| Oren-Nayar | 3 | non linear |
| RPV | 4 | non linear |
| Ross-Li | 3 | linear |
| Ross-Li-HS | 3 | linear |
| Ross-Li-HS-desert | 3 | linear |
| Roujean | 3 | linear |
| Roujean-HS | 3 | linear |
| Snyder | 7 | non linear |
| Walthall | 4 | linear |

- **Fitting performances of BRDF models over laboratory measurements**
  - Estimation of the model parameters using:
    - The whole set of available angles (no measurement in the backscattering direction)
    - 20 initial conditions generated randomly
    - The one giving the minimum rms error is selected among the twenty
  - Estimation for the 6 wavelengths of PARASOL + 1600 and 2200 nm independently
  - Comparison of 5 models: Snyder, RPV, Roujean, Oren-Nayar and Ross-Li Maignan
  - Best results for Snyder and RPV whatever the sample

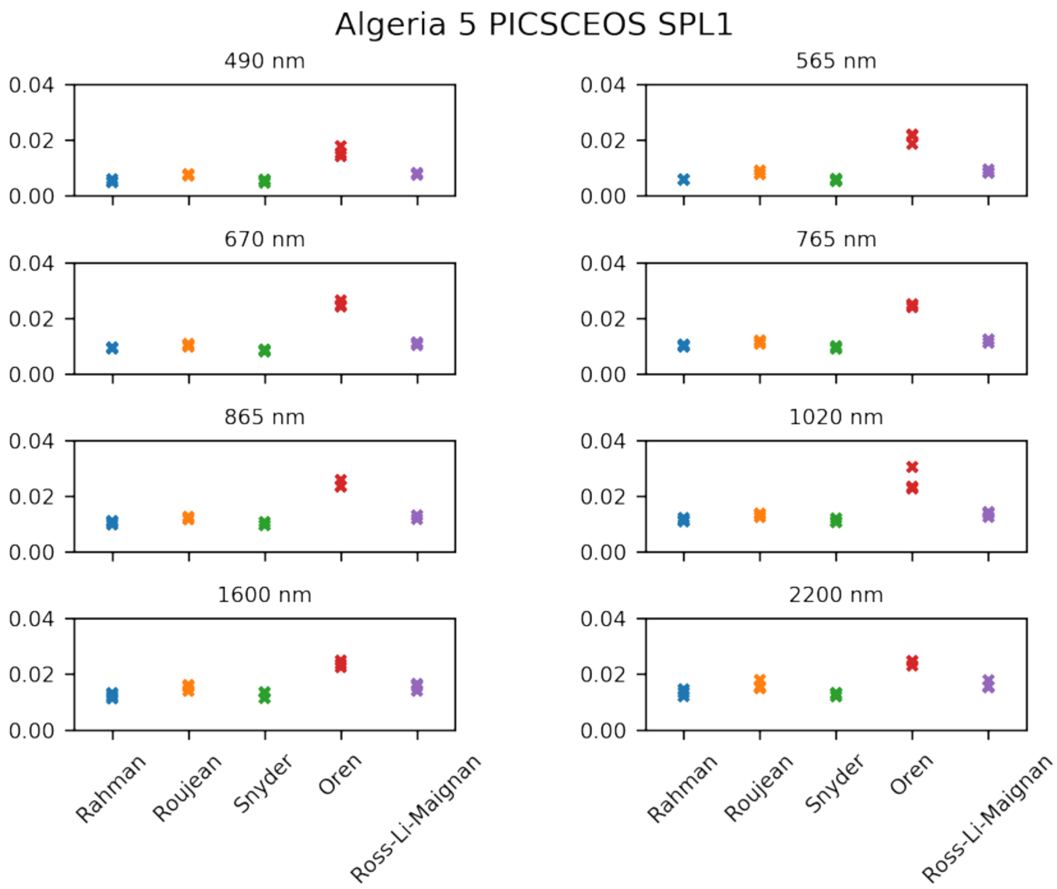


Algeria5_PICSCEOS SPL1 residual RMSE between the measured BCRF for the three rotating positions and the 5 fitted BRDF models (Note that Ross-Li-Maignan = Ross-Li-HS).

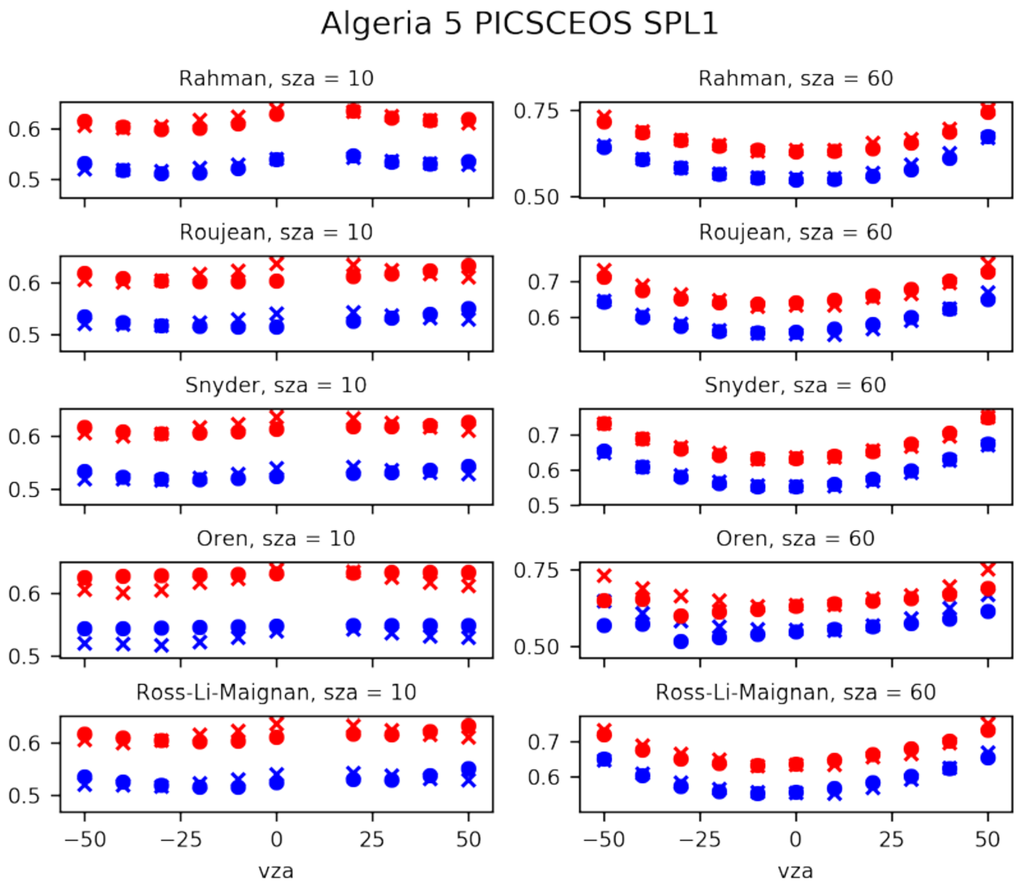
Algeria 5 PICSCEOS SPL1
Rahman, sza = 10
Rahman, sza = 60
Roujean, sza = 10
Roujean, sza = 60
Snyder, sza = 10
Snyder, sza = 60
Oren, sza = 10
Oren, sza = 60
Ross-Li-Maignan, sza = 10
Ross-Li-Maignan, sza = 60
0.6
0.5
0.75
0.50
0.7
vza
−50
−25
0
25
50

# Fitting performances over PARASOL data

## Optimization procedure

- **linear models**: minimization of the RMS difference between measurements and model outputs using a simple matrix inversion.
- **non-linear models**: a non-linear least square optimization approach was used, several first guess parameter sets

## Data used

- monthly data / each of the 6 PARASOL band ➔ monthly model
- yearly data (assumes temporal stability) ➔ yearly model

Algeria 5
Monthly model

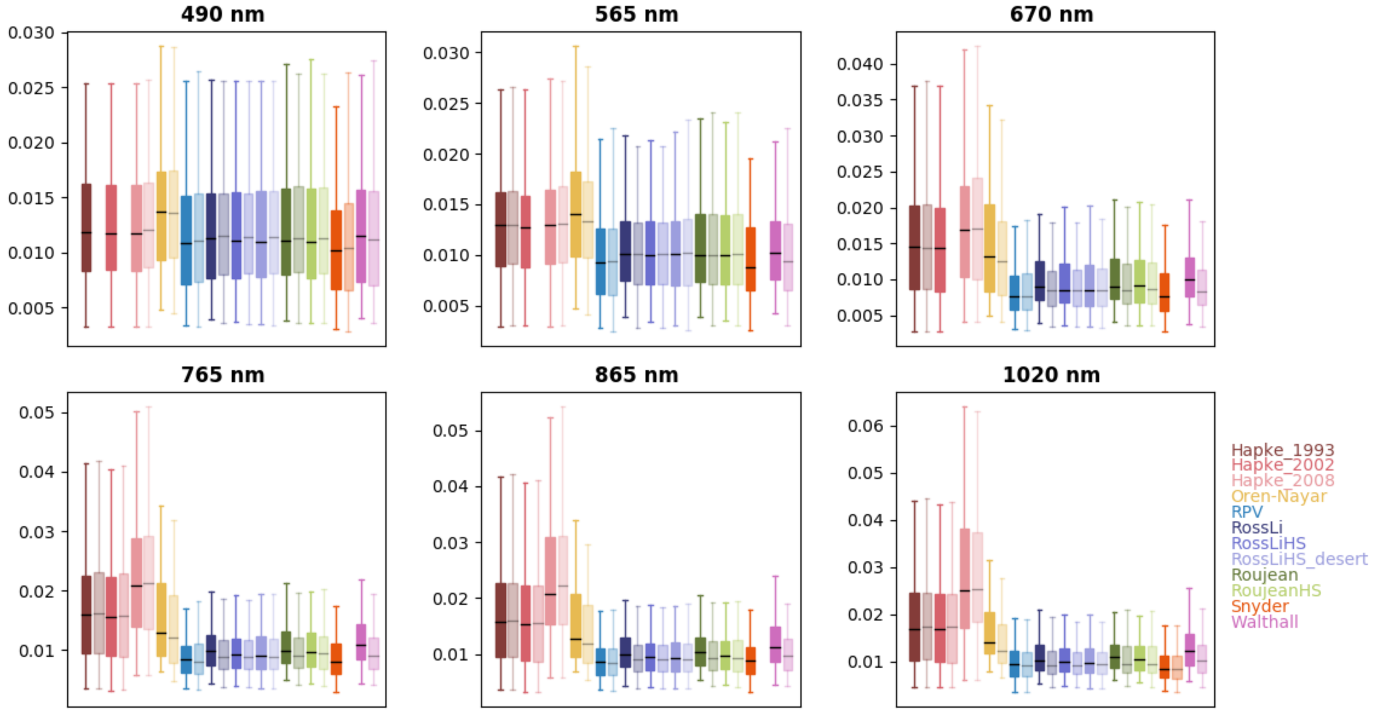

# Algeria 5

## Yearly model

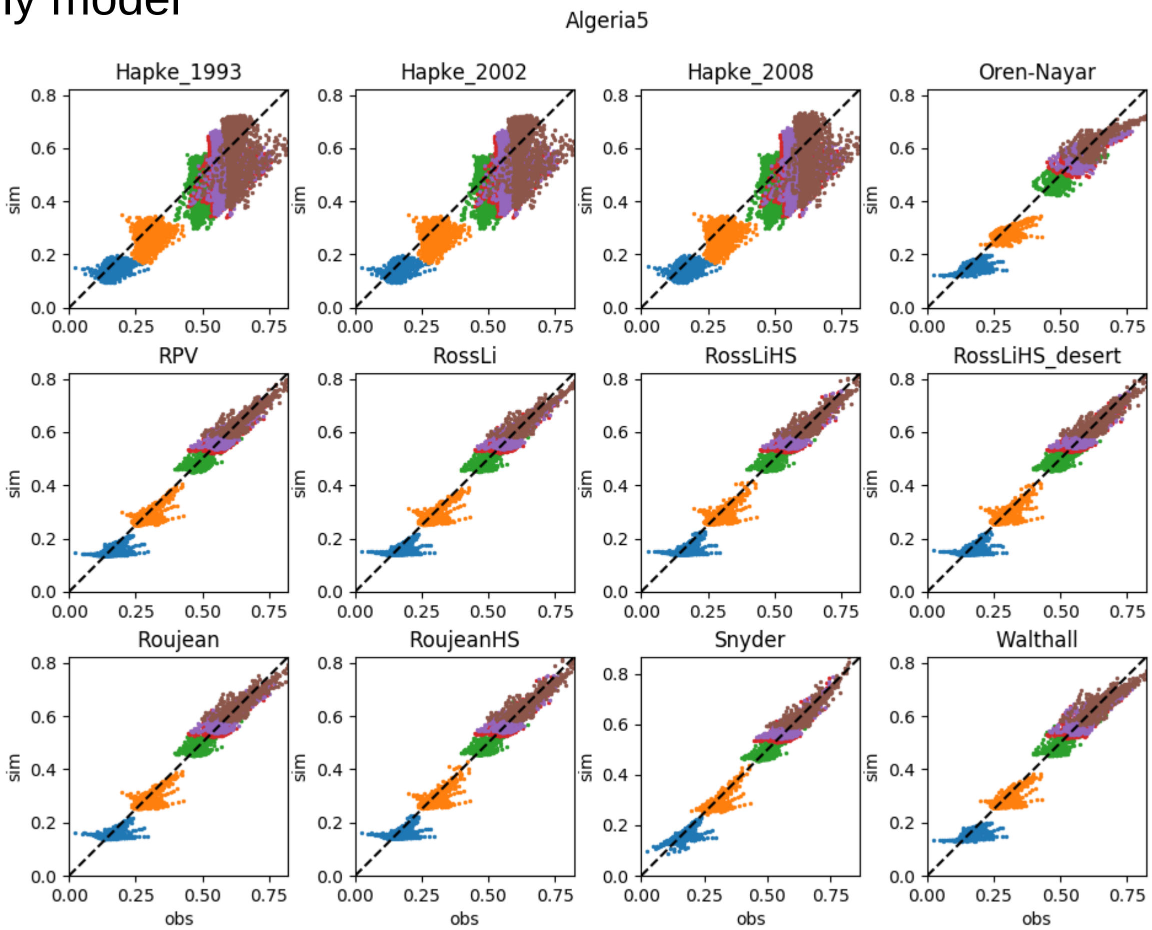

## Algeria 5
### Yearly model

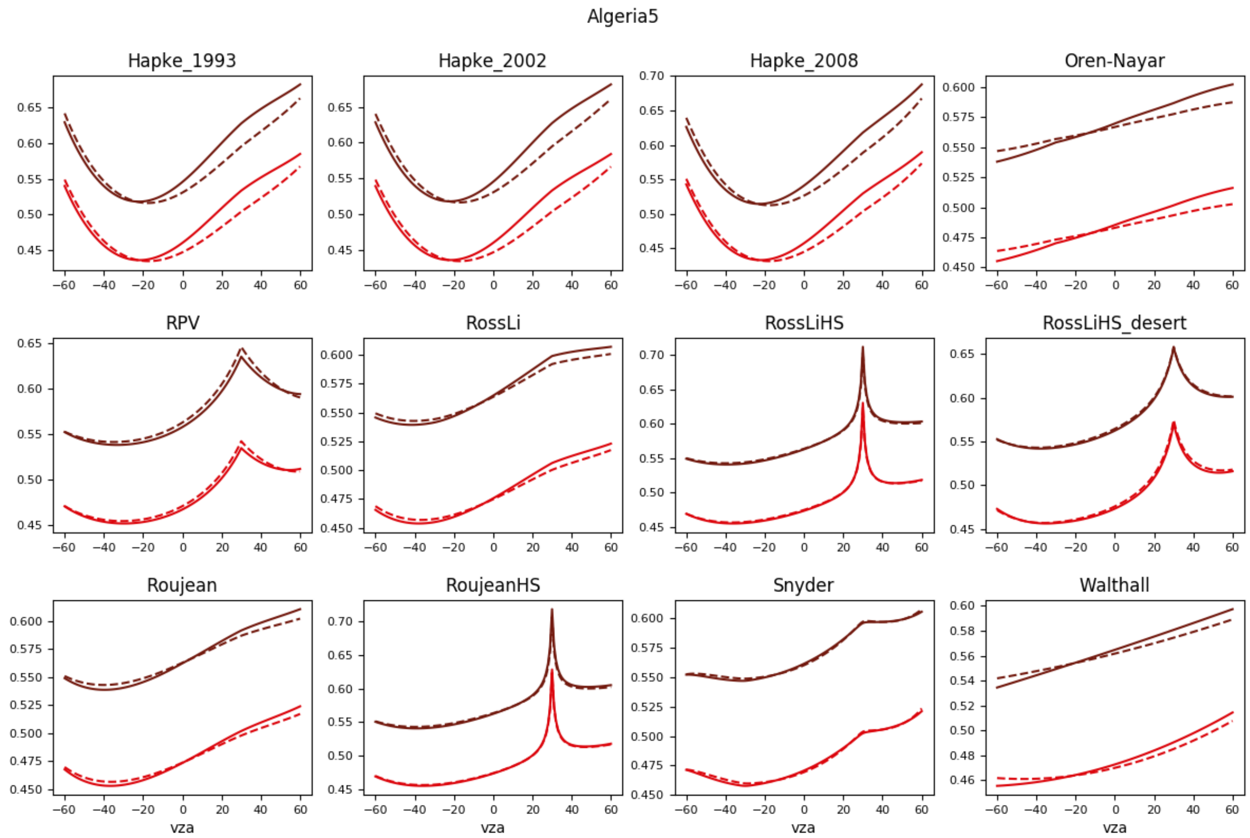


*plain lines: all data accounted for*
*dashed lines: data around the hot spot discarded*

## Synthesis

- Similary ranking between laboratory / space-borne data
- Best models RPV and Snyder
  - PARASOL: RPV > Snyder for the calibration of the yearly models
- Followed closely by Ross-Li-HS, Ross-Li/Roujean
- Poorer performances with Oren-Nayar and Hapke
- Some convergence issues with Snyder and Hapke

- Discrepancies between models in the way the reflectance in the hot spot and in backscatter directions is modelled

- The fitting performances should also be weighted with regards to the number of parameters of the model: 7 for Snyder model, 4 for RPV, 3 for the “simpler” models like the Ross-Li or Roujean (and versions derived from them).

# Outline

- Context & objectives
- Sites selection process
- Surface characterization
- **Atmospheric characterization**
- PICSAND Data Base
- Conclusion

# Variables and datasets

## AOD and cloud coverage

- MYD04_L2 (collection 6) **2003-2015** (without 2013) – 16days / 10kmx10km: AOD and cloud fraction
- nebulosity map (CNES) from ECMWF weather data
- MACC re-analysis - over the 2003-2012: AOD by aerosol types

## Trace gases ($O_3$, $H_2O$)

- MYD08_M3 (coll 6): **2003-2015**; monthly / 1° x1° (also AOD and CF)

## Weather data

- Tair, Psurf, Air specific humidity, Wind speed, SWdown, LWdown
- CRU-NCEP: 6h / 0.5° x 0.5° : **1989-2012**
- ERA-I: 3h / 0.7° x 0.7° : **1989-2012**
- CERA-SAT: 3h / 0.7° x 0.7° : **2008-2016**

➔ **Monthly climatologies for all sites**

- **Monthly aerosol optical depth and cloud fraction derived from MYD04_L2 (collection 6) over 2003-2015, and nebulosity from ECMWF weather data (072012-06/2013). The blue line is the mean value calculated from all data-month; the grey area is the standard deviation; orange and green lines correspond to the 10th and 90th of the distribution of the values for each month**

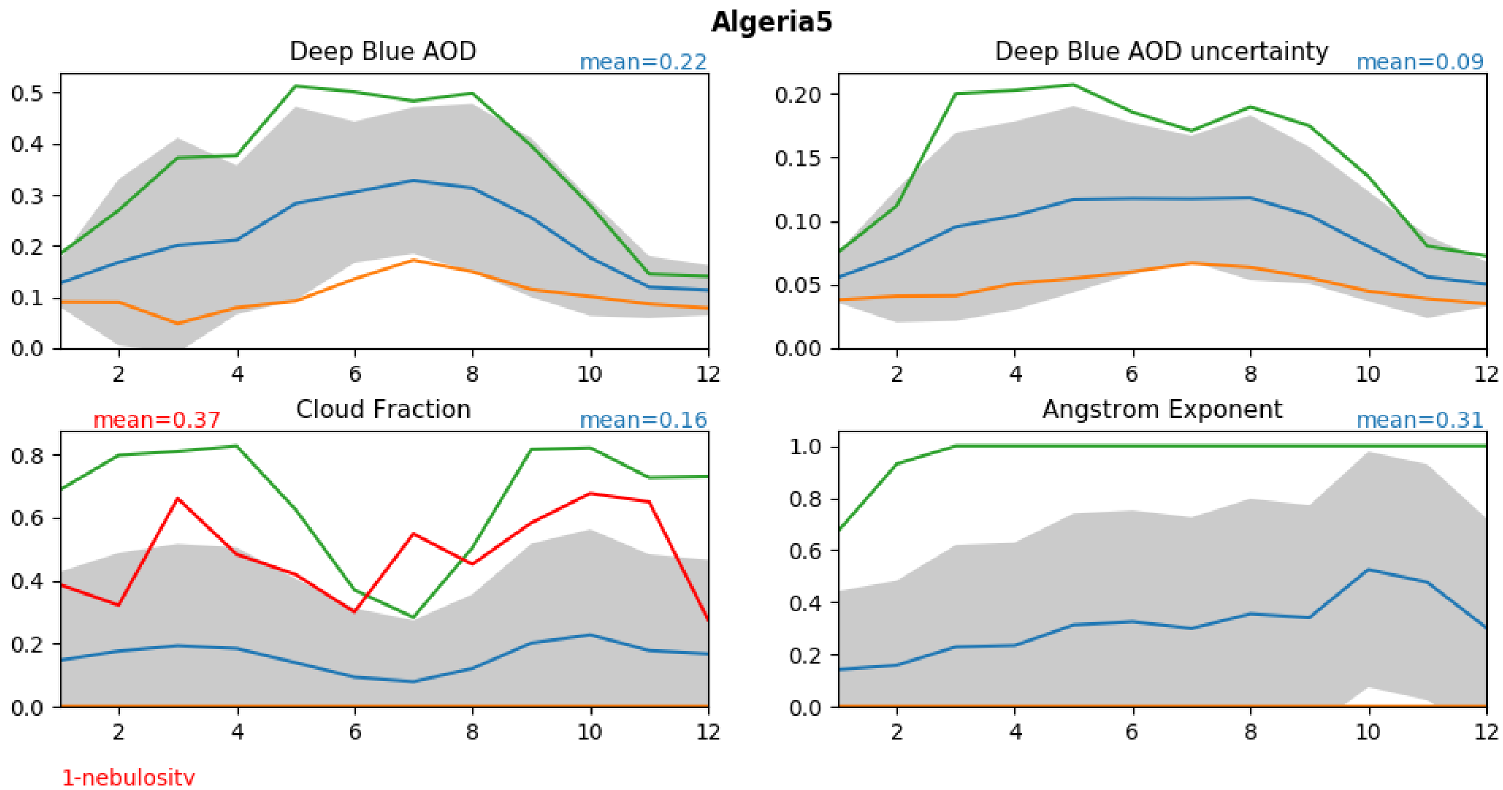

- **Monthly climatology of total column of O3 and H2O, as well as AOD and cloud fraction (daytime observations only) derived from MYD08_M3 over 2003-2015.**
- **The blue line is the mean value calculated from all data-month; the grey area is the standard deviation; orange and green lines correspond to the 10th and 90th of the distribution of the values for each month**

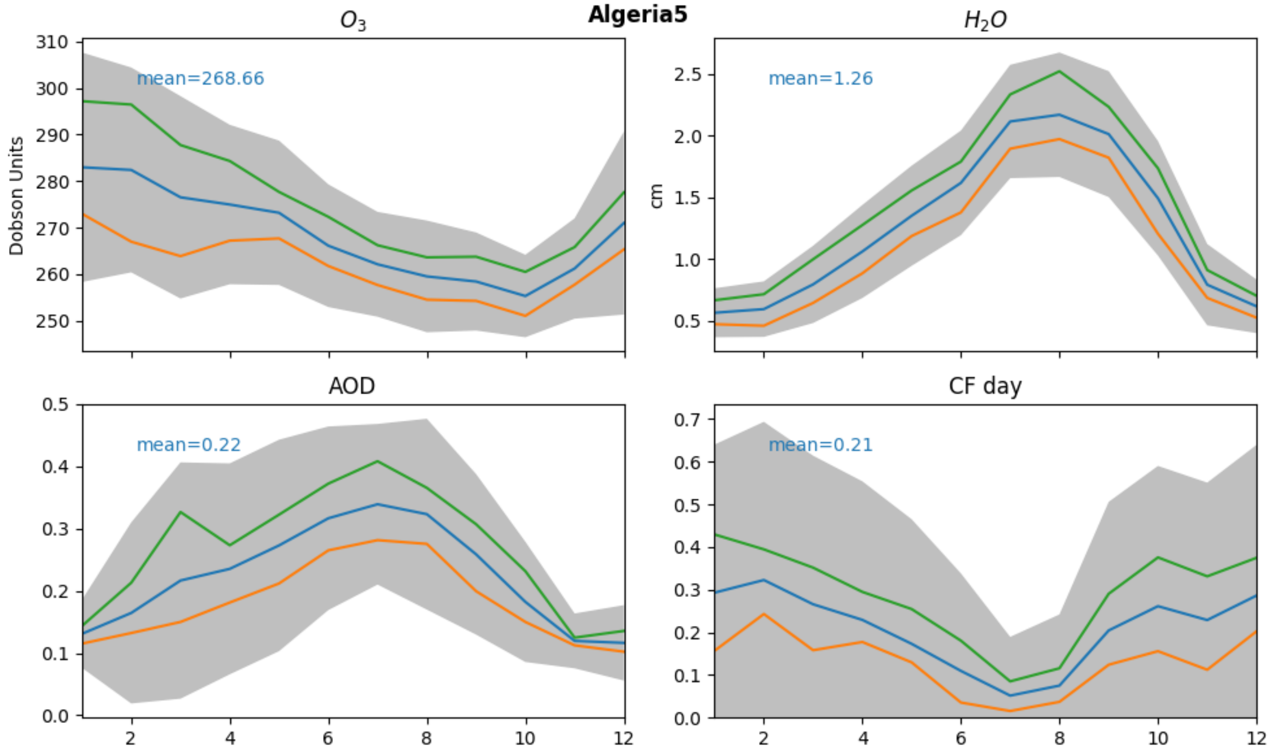

# Climatology

- **Monthly climatology of AODs (total and for dust, organic matter, sea salt, black carbon, sulphat, aerosols), derived from daily MACC re-analysis over 2003-2012**
- **The blue line is the mean value calculated from all data-month; the grey area is the standard deviation; orange and green lines correspond to the 10th and 90th of the distribution of the values for each month.**
- **The relative contribution of each aerosol type to the total AOD is also provided (calculated as the mean ratio of the AOD associated to the type considered to the total AOD).**

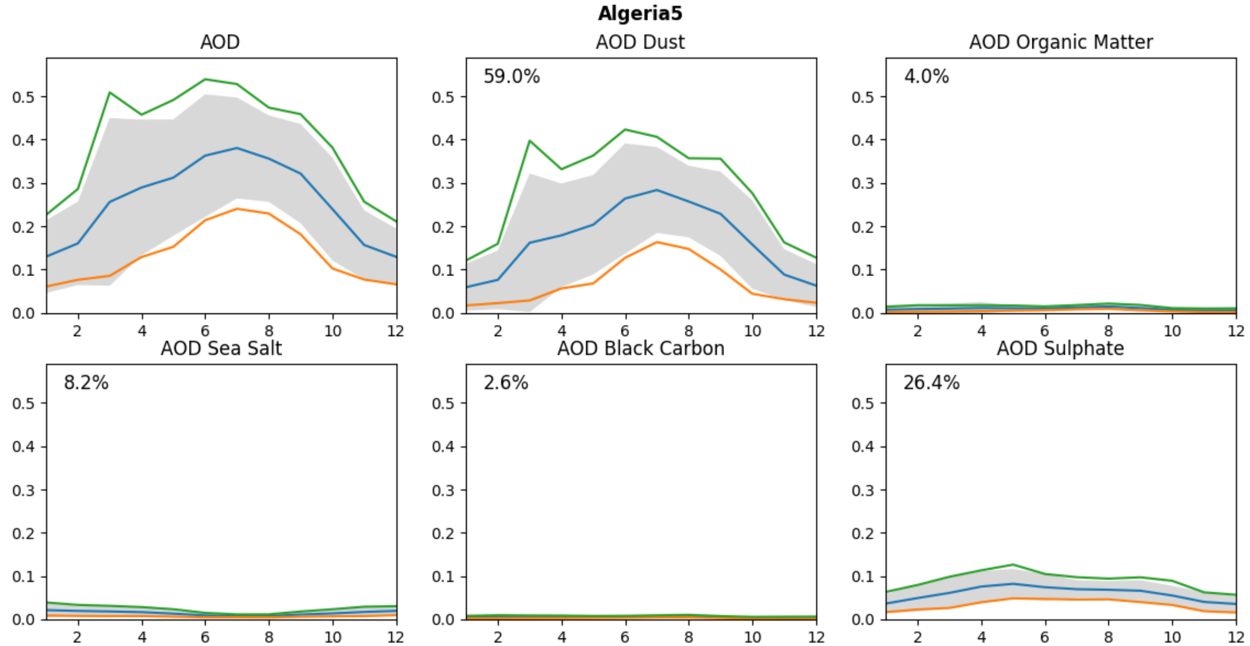

# Weather data

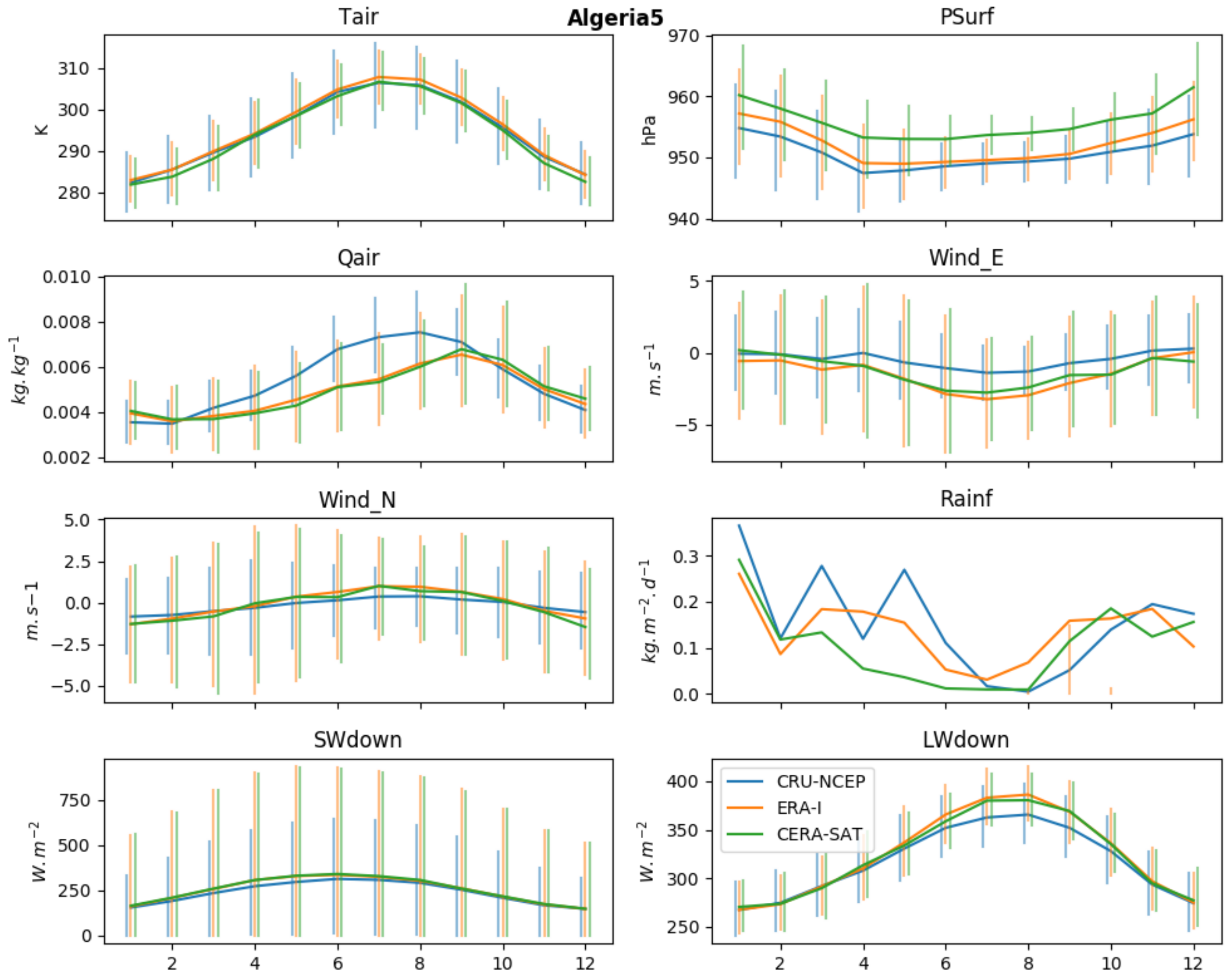

# Outline

- Context & objectives
- Sites selection process
- Surface characterization
- Atmospheric characterization
- **PICSAND Data Base**
- Conclusion

# PICSAND Data Base

- **https://picsand.noveltis.fr/**

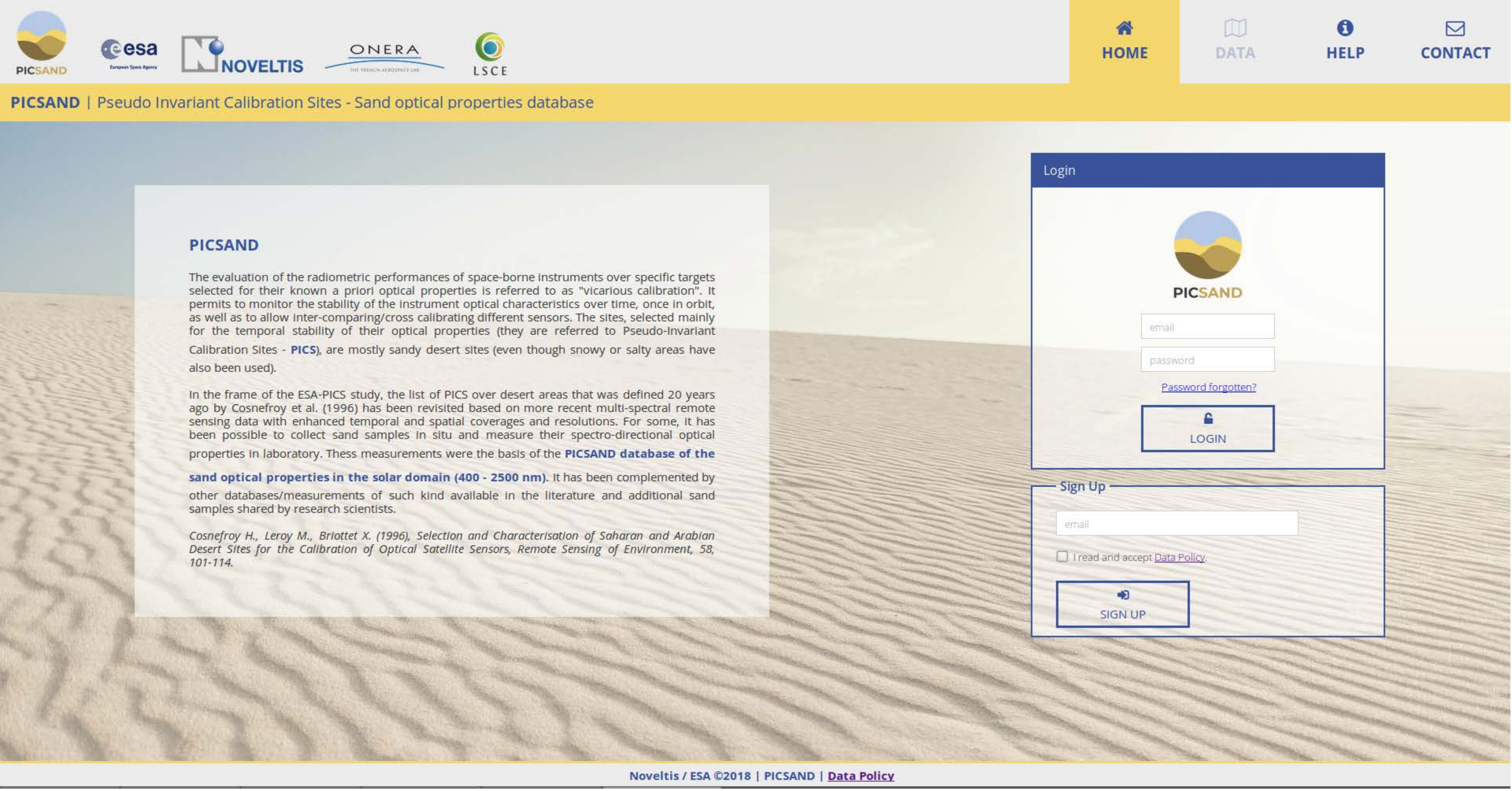

- **https://picsand.noveltis.fr/**

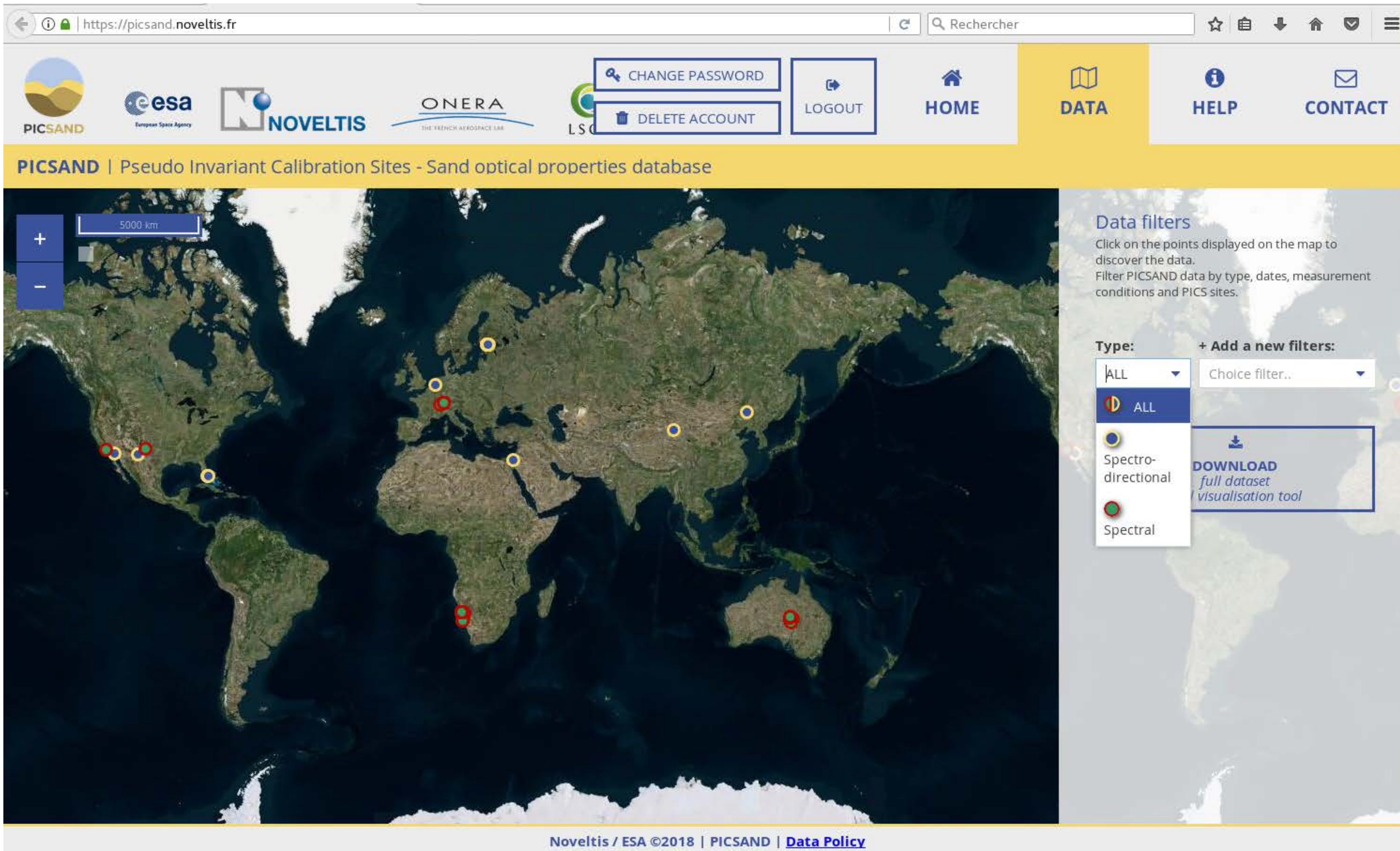

# PICSAND Data Base

- **https://picsand.noveltis.fr/**

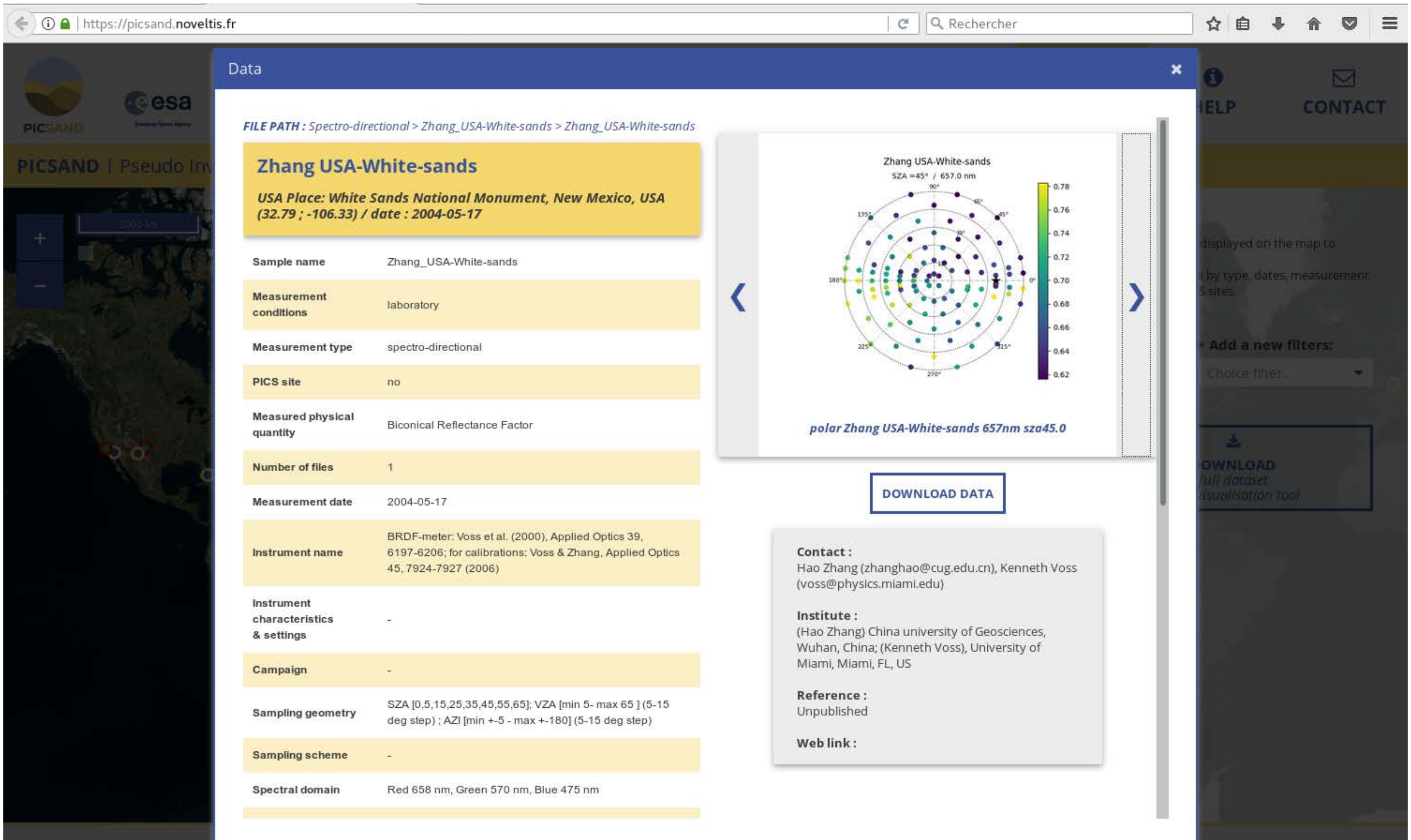

# Content

- Spectral-BRF / spectral measurements performed by ONERA
  - Sand collected for some PICS sites + Other sand samples
  - Available after publication
- Measurements available from the literature

## spectro-directional data

| PI | Country | Characteristics | Spectral Domain |
|---|---|---|---|
| **ONERA** | France | Algier / Narbonne | 520-910 nm |
| **ONERA** | Algeria | Algeria3 / Algeria5 | 350-2500 nm |
| **ONERA** | Morocco | Erg Chebbi | |
| **ONERA** | Namibia | RadCalNet site / Gobabeb | |
| **ONERA** | Arabia | ArabiaPICS2 | |
| **ONERA** | Niger | Niamey | |
| **ONERA** | Libya | Erg Ubaru | |
| **Cierniewski - Karnieli** | Israel | Negev | 450, 550, 650, 850,1650 nm |
| **Coburn** | USA | Algodones Dunes | 400-900 nm |
| **Peltoniemi** | Finland | beach, football, car park | 350-2500 nm |
| **Roosjen** | Netherlands | sand, sandy loam | 350 - 2499 nm |
| **Sun** | China | Xianjiamu Sumu / 3 grain size | 400 - 2500nm |
| **Zhang/Voss** | USA | sand beach + White sands | 475, 658 nm |
| **Zhang** | China | Dunhuang site | 399-2386 nm |

## spectral data

| PI | Country | Characteristics | Spectral Domain |
|---|---|---|---|
| **ONERA** | Libya | Fezzan Fez | 350-2500 nm |
| **ONERA** | Australia | Lucky Bay / Pinnacle / Wylie Bay | |
| **ONERA** | USA | RailRoad Valley playa / White Sands | |
| **ONERA** | Namibia | | |
| **ASTER** | | | 400 – 14011 nm |
| **USGS** | USA | | 350 - 2500 nm |
| **Hueni** | Swiss | sand (bright, coarse, fine, dark..) | 350 – 2500 nm |
| **NPL** | Namibia | different soil colours | 380 – 2500 nm |
| **White, Bullard** | Australia | Simpson Desert | 400 - 2500 nm |
| **White, Bullard** | Namibia | | 400 - 2500 nm |
| **White, Bullard** | USA | Muleshoe Dunes | 400 - 2500 nm |

# Access

- https://picsand.noveltis.fr/
- User requested to agree to a Data Use Policy
  - properly reference the datasets
- Online portal hosted on the CEOS/IVOS portal: http://calvalportal.ceos.org/pics
- ONERA measurements will be available after publication
- Download of the data:
  - by dataset
  - all data + Python tool to help reading/displaying the data

# Outline

- Context & objectives
- Sites selection process
- Surface characterization
- Atmospheric characterization
- PICSAND Data Base
- **Conclusion**

# Conclusion

- Recommendations:
  - PICS location
    - Keep the original Cosnefroy's sites as the reference calibration targets
      - optimal locations are found close enough to the initial sites
      - their scrore is only slightly better than the orginal PICS
      - importance of the Cosnefroy sites for Cal/Val activities over the last 20 years
    - Redo the exercise for smaller spatial and/or temporal scales:
      - smaller sites suited to HR sensors
      - sites relevant for a limited period of the year.
  - Climatology of aerosols and cloud cover
    - Take it into account for selecting the most relevant sites as well as the acquisition period suited to the sensor to calibrate.
  - Surface characterization
    - Use preferably RPV or Snyder BRDF (if enough observations are available) models

# Conclusion

- Study ended
- Operational Data Base
- Writing of 2 papers in progress
- Proposal submitted for:
  - Enhancement of reliability and traceability of BCRF measurements through more suited reference panels (spectralon) characterization
  - Possibility of adding data in the PICSAND data base

Thanks for your attention !